Journal of
Applied Crystallography
ISSN 0021-8898

Received 29 December 2009
Accepted 6 May 2010

Hexagonal and cubic $TiOF_2$

Samuel Shian[a] and Kenneth H. Sandhage[a,b]*

[a]School of Materials Science and Engineering, Georgia Institute of Technology, Atlanta, GA 30332, USA, and [b]School of Chemistry and Biochemistry, Georgia Institute of Technology, Atlanta, GA 30332, USA. Correspondence e-mail: ken.sandhage@mse.gatech.edu

The chemical, electrochemical, optical and electro-optical properties of titanium oxyfluoride, $TiOF_2$, have led to interest in this compound for a number of applications. Prior analyses have indicated that $TiOF_2$ possesses a simple cubic structure (space group $Pm\bar{3}m$) at room temperature. Three-dimensional nanostructured assemblies of polycrystalline $TiOF_2$ have recently been synthesized *via* chemical conversion of intricate SiO_2 structures by metathetic reaction with TiF_4(g). Rietveld analysis has been used to evaluate the structure of the $TiOF_2$ product formed by such reaction at 623 K. Unlike prior reports, this $TiOF_2$ product possessed a hexagonal structure (space group $R\bar{3}c$) at room temperature. Upon heating through 333–338 K, the hexagonal $TiOF_2$ polymorph converted into cubic ($Pm\bar{3}m$) $TiOF_2$. Differential scanning calorimetry and X-ray diffraction analyses have been used to evaluate this thermally induced phase transformation.

1. Introduction

Titanium oxyfluoride, $TiOF_2$, has chemical, optical, electrochemical and electro-optical properties that can be attractive for use in catalysis/photocatalysis (Tanuma *et al.*, 2010; Zhu *et al.*, 2009), UV-absorbing cosmetics, paint or glass (Demourgues & Kempf, 2003), lithium ion batteries (Reddy *et al.*, 2006), and electrochromic displays and windows (Gutarra *et al.*, 1994). Titanium oxyfluoride is also a component of, or a reactant used in the syntheses of, other functional oxyfluoride-bearing materials (Poulain & Poulain, 1991; Grannec *et al.*, 1988; Guelin *et al.*, 1988).

In 1955, Vorres & Donohue evaluated the crystal structure of titanium oxyfluoride generated by the hydrolysis of titanium tetrafluoride (TiF_4) or titanium trifluorochloride (TiF_3Cl), or by the reaction of hydrogen fluoride with titanium dioxide (Vorres & Dutton, 1955). The room temperature X-ray powder diffraction pattern of $TiOF_2$ was found to be consistent with a simple cubic crystal structure (Vorres & Donohue, 1955). More recently, gas/solid metathetic reactions of the following type have been suggested for converting silica structures into replicas composed of other materials (Sandhage *et al.*, 2002; Sandhage, 2006):

$$2TiF_4(g) + SiO_2(s) \rightarrow 2TiOF_2(s) + SiF_4(g). \qquad (1)$$

Nanostructured $TiOF_2$ replicas of the intricate three-dimensional SiO_2 microshells of diatoms, a type of unicellular algae, have been generated through such metathetic reactive conversion at $\leq$623 K (Unocic *et al.*, 2004; Sandhage, 2006; Lee *et al.*, 2007). A similar reaction process has been used to convert SiO_2 microspheres and three-dimensional ordered macroporous SiO_2 templates into $TiOF_2$ replicas (Shian & Sandhage, 2009; Lytle *et al.*, 2004). However, room-temperature X-ray diffraction analyses of the $TiOF_2$ formed by such a TiF_4(g)/SiO_2(s) reaction yielded diffraction patterns that were not consistent with the cubic crystal structure reported by Vorres & Donohue. The purpose of this paper is to evaluate the crystal structure of these $TiOF_2$ replicas, both at room temperature and upon modest heating (up to 423 K).

2. Experimental

2.1. Reaction processing of $TiOF_2$

Titanium oxyfluoride was synthesized *via* the reaction of silica microspheres with titanium tetrafluoride gas generated inside sealed titanium ampoules. SiO_2 microspheres (>99.9% purity, 1 µm diameter, Fiber Optic Center Inc., New Bedford, Massachusetts, USA) and solid TiF_4 powder (99% purity, Advanced Research Chemicals Inc., Catoosa, Oklahoma, USA) were placed within a titanium tube of 2.3 cm inner diameter and 20 cm length (ASTM B338 Grade 2 titanium, McMaster–Carr, Atlanta, Georgia, USA). Both ends of the tube were then crimped and welded shut. The molar TiF_4:SiO_2 reactant ratio sealed within the tube was 2.4:1 [*i.e.* in excess of the reactant stoichiometry indicated by reaction (1)]. The storage, weighing and titanium ampoule sealing of the solid titanium tetrafluoride and silica spheres were conducted within a high-purity argon atmosphere glove box (Model Omni-Lab, Vacuum Atmosphere, Hawthorne, California, USA) maintained at an oxygen partial pressure below 0.1 p.p.m.

The sealed metal ampoules were heated to 623 K at a rate of 5 K min^{-1}, held at 623 K for 4 h, and then cooled at 15 K min^{-1} to room temperature. The ampoules were then cut open and the reacted specimens were extracted for characterization.

2.2. $TiOF_2$ characterization

Secondary-electron images and chemical analyses of the titanium oxyfluoride specimens were obtained with a field-emission scanning electron microscope (LEO-1530, Carl Zeiss, Oberkochen, Germany) equipped with energy-dispersive X-ray analysis capability (Oxford Instruments, Buckinghamshire, UK). Differential scanning calorimetry (DSC) analyses were conducted in ambient air at heating and cooling rates of 10 K min^{-1} (DSC-60 calorimeter, Shimadzu Corporation, Kyoto, Japan).

Room-temperature X-ray diffraction (XRD) analysis was performed in ambient air with a diffractometer configured for Bragg–Brentano geometry (X'Pert PRO Alpha-1 diffractometer, PANalytical, Almelo, The Netherlands). A symmetrical Johansson monochromator restricted the incident X-ray beam to the $K\alpha_1$ component of Cu radiation. Peak-profile data acquisition was conducted with a solid-state position-sensitive detector (X'Celerator, PANalytical). A divergence slit of 0.25° and a 0.02 radian Soller slit were used in the incident beam path. A 0.02 radian Soller slit and a 5 mm antiscattering slit were used in the diffracted beam path.

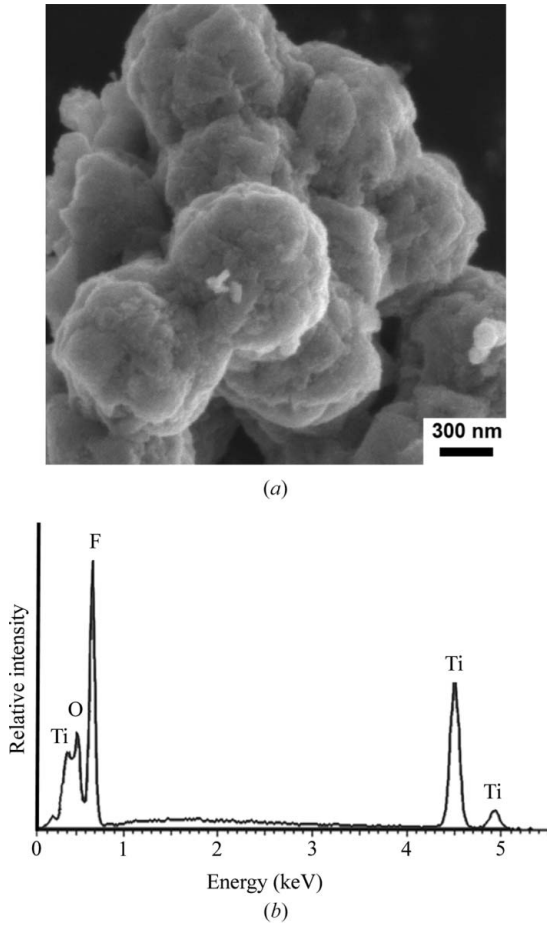

Figure 1
(*a*) Secondary-electron image of the $TiOF_2$ product generated by reacting SiO_2 microspheres with TiF_4(g) at 623 K for 4 h. (*b*) EDX analysis of this product, revealing appreciable amounts of titanium, oxygen and fluorine, and the absence of silicon (*e.g.* the Si $K\alpha_1$ peak at 1.74 keV is missing).

Table 1
Crystallographic data for hexagonal $TiOF_2$ synthesized by the reaction of SiO_2 with TiF_4(g) at 623 K.

Space group	$R\bar{3}c$ (No. 167)
Unit cell	a = 5.3325 (1) Å
	c = 13.2321 (4) Å
Atom coordinates	Ti (0, 0, 0), occupancy = 1
	F [0.5486 (5), 0, $\frac{1}{4}$], occupancy = $\frac{2}{3}$
	O [0.5486 (5), 0, $\frac{1}{4}$], occupancy = $\frac{1}{3}$
Rietveld statistics	R_{exp} = 9.86, $R_{weighted\ profile}$ = 12.62, χ^2 = 1.64

XRD analyses at elevated temperature were conducted with a diffractometer configured for Bragg–Brentano geometry (X'Pert PRO MPD diffractometer, PANalytical) that was equipped with a furnace (HTK 1200, Anton Paar, Graz, Austria). The converted $TiOF_2$ was heated to the desired temperature, in the range 298–423 K, for subsequent diffraction analysis in ambient air. Diffraction patterns were obtained using Cu $K\alpha$ X-rays. A W/Si multilayered focusing (Göbel) mirror was attached to the incident beam path to create a high-intensity parallel beam for a high signal-to-noise ratio. A divergence slit of 0.5° was used in the incident beam path. Peak-profile data acquisition was conducted with a solid-state position-sensitive detector (X'Celerator, PANalytical). A 0.02 radian Soller slit and a 5 mm antiscattering slit were used in the diffracted beam path.

Rietveld refinements of the XRD data were performed using *X'Pert Highscore Plus* software (PANalytical, 2006). The X-ray data were fitted using the pseudo-Voigt profile function. The specimen displacement, polynomial coefficients for the background function, lattice parameters, profile parameters, and Gaussian and Lorentzian profile coefficients were refined. The atomic coordinates of titanium were fixed, and the coordinates of both fluorine and oxygen anions were allowed to converge. The refined structures were visualized using *JADE* software (Materials Data, 2007).

3. Results and discussion

3.1. Room-temperature crystal structure of $TiOF_2$

A secondary-electron image of the polycrystalline $TiOF_2$ reaction product is shown in Fig. 1(*a*). Energy-dispersive X-ray (EDX) analyses of this product (Fig. 1*b*) reveals the presence of appreciable levels of titanium, fluorine and oxygen, and the absence of silicon, which is consistent with the complete conversion of SiO_2 into $TiOF_2$ within 4 h at 623 K. The powder XRD pattern obtained at room temperature from this product is shown in Fig. 2. All of the detected peaks could be indexed on the basis of a hexagonal (or rhombohedral) unit cell. The results of Rietveld refinement of this XRD pattern are shown in Table 1, and the associated structure is illustrated in Figs. 3(*a*) and 3(*c*).[1] The hexagonal $TiOF_2$ structure (space group $R\bar{3}c$) consists of Ti atoms octahedrally coordinated by randomly distributed O and F atoms. The TiO_2F_4 octahedra

[1] Supplementary data for this paper are available from the IUCr electronic archives (Reference: CE5082). Services for accessing these data are described at the back of the journal.

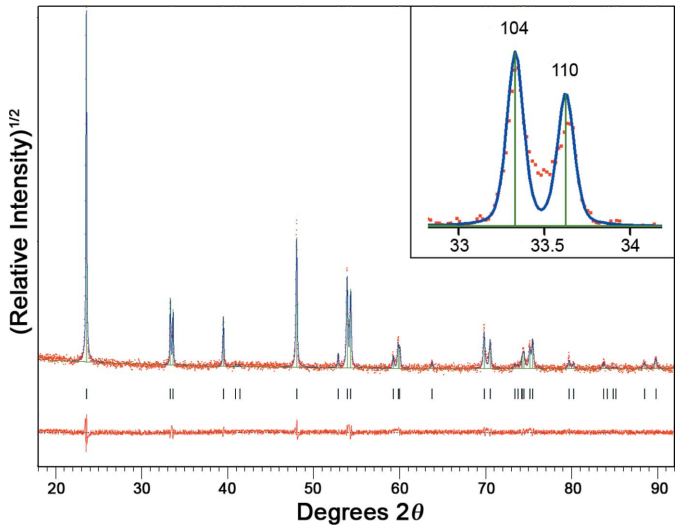

Figure 2
Rietveld refinement (shown as a continuous line) of the room-temperature XRD pattern obtained from $TiOF_2$ (shown as dots). Allowed reflections for the $R\bar{3}c$ space group are indicated with tick marks. The profile of the difference between the experimental data and the refined pattern is shown below the tick marks. The inset image reveals a magnified view of the data and the associated Rietveld fit for the (104) and (110) reflections for the $R\bar{3}c$ space group. [Note that, for the $Pm\bar{3}m$ space group, a single (011) peak would be located within this 2θ range.]

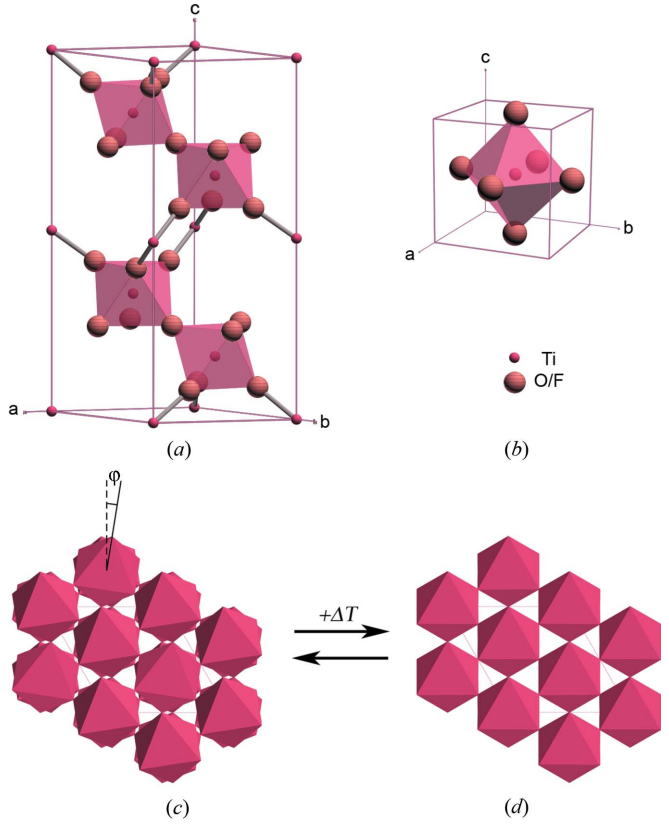

Figure 3
(*a*) Hexagonal $TiOF_2$ unit cell (space group $R\bar{3}c$). (*b*) Cubic $TiOF_2$ unit cell (space group $Pm\bar{3}m$). (*c*) TiO_2F_4 octahedra in hexagonal $TiOF_2$, viewed down the $[001]_{hexagonal}$ direction. The octahedral tilt angle is shown as φ. (*d*) TiO_2F_4 octahedra in cubic $TiOF_2$, viewed down the $[111]_{cubic}$ direction.

share all six corners with neighboring octahedra. Each unit cell contains six $TiOF_2$ molecules. The calculated theoretical density and Ti—X distances are 3.114 Mg m^{-3} and 1.911 Å, respectively. This hexagonal $TiOF_2$ structure is closely related to the previously reported cubic ReO_3-type structure of $TiOF_2$ (Vorres & Donohue, 1955; Hayward *et al.*, 2005; ICDD, 2007). The cubic $TiOF_2$ structure (space group $Pm\bar{3}m$), illustrated in Figs. 3(*b*) and 3(*d*), also consists of a three-dimensional network of corner-sharing TiO_2F_4 octahedra. However, each of the TiO_2F_4 octahedra in the hexagonal structure rotates around one of the triad axes of the cubic phase, in a manner categorized by Glazer (1972) as the $a^-a^-a^-$ tilt system. All octahedra tilt through an angle (shown as φ in Fig. 3*c*) of similar magnitude, with half of the octahedra rotating clockwise around the triad axis and the other half rotating counterclockwise (Hayward *et al.*, 2005). Such tilting results in a distortion (elongation or contraction) of the TiO_2F_4 octahedra along the rotation axis.

3.2. Hexagonal to cubic $TiOF_2$ phase transformation

XRD patterns obtained upon heating and cooling of the $TiOF_2$ are shown in Fig. 4. A gradual decrease in the intensities of several hexagonal reflections, such as the (113) reflection near 2θ = 39.4° and the (211) reflection near 2θ = 52.8° (not shown), was observed upon heating. Such heating also resulted in the convergence of closely located hexagonal reflections, such as the (104) and (110) reflections near 2θ = 33.3 and 33.6°, respectively, and the (116) and (122) reflections

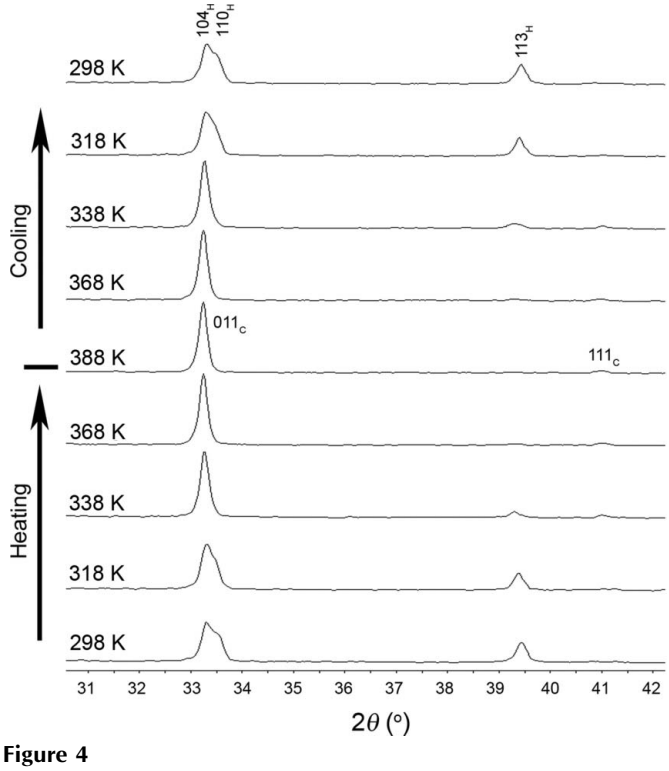

Figure 4
Diffraction patterns of $TiOF_2$ in a selected 2θ range upon heating and cooling. The progressive reversible transition between the hexagonal (subscript H) and cubic (subscript C) $TiOF_2$ structures can be observed.

near $2\theta = 53.9$ and 54.3°, respectively (not shown), into single reflections. These gradual changes are an indication of the TiO_2F_4 octahedra rotating from the lower $R\bar{3}c$ (hexagonal) symmetry toward the higher $Pm\bar{3}m$ (cubic) symmetry upon heating. Diffraction patterns collected above 338 K exhibited only reflections associated with cubic ($Pm\bar{3}m$) $TiOF_2$. The unit-cell lattice parameter of cubic $TiOF_2$ reported by Vorres & Donohoe ($a = 3.798$ Å) at room temperature is quite similar to the unit-cell parameter of $TiOF_2$ obtained at 368 K ($a = 3.806$ Å) in the present work. Upon cooling, the cubic $TiOF_2$ polymorph was observed to convert back into hexagonal $TiOF_2$.

DSC analyses (Fig. 5) indicated that the hexagonal-to-cubic transformation of $TiOF_2$ was endothermic. The onset of the transformation, determined from changes in the slopes of the DSC curves during heating and cooling, was found to occur at about 333–338 K. The molar enthalpy change of transformation, $\Delta H^{H\rightarrow C}$, was determined to be 0.11 kJ mol^{-1}. These values of onset temperature and enthalpy of transformation are similar to those reported for the hexagonal-to-cubic transformation of titanium trifluoride, TiF_3. Calorimetric studies by Mogus-Milankovic *et al.* (1985) and Daniel *et al.* (1990) yielded transition temperatures of 340 (10) K and 338–344 K, respectively, and enthalpies of transformation of 0.22 and 0.44 J mol^{-1}, respectively.

XRD analysis of the change in the $TiOF_2$ unit-cell volume during heating through the hexagonal-to-cubic transformation is shown in Fig. 6. The unit-cell volume increased more rapidly with heating below, rather than above, the transformation temperature; that is, the volumetric thermal expansion coefficient of hexagonal $TiOF_2$ was noticeably higher than for cubic $TiOF_2$. Changes in the unit-cell lattice parameters with temperature are shown in Fig. 7. Upon heating, the a and c lattice parameters for hexagonal $TiOF_2$ increased and decreased, respectively, with a more dramatic change with temperature observed for the a lattice parameter. Calculated for cubic equivalence, the values of the a and c lattice parameters eventually merged upon completion of the transformation from hexagonal to cubic $TiOF_2$. The TiO_2F_4 octahedral tilt angle (φ) in hexagonal $TiOF_2$ was also evaluated using the equation (Howard *et al.*, 2000)

$$\tan\varphi = 2(x - 1/2)3^{1/2}, \qquad (2)$$

where x refers to the position of a given anion, $(x, 0, \frac{1}{4})$, in the hexagonal unit cell. At room temperature, the octahedral tilt angle was about 9°. As the temperature increased (Fig. 8), the octahedral tilt angle decreased progressively until, upon complete conversion to the cubic phase, the value fell to zero.

The gradual changes observed in the $TiOF_2$ unit-cell volume, lattice parameters and octahedral tilt angle with increasing temperature were consistent with a continuous transition upon heating. Similar gradual changes in structure have been reported for the thermally induced hexagonal-to-

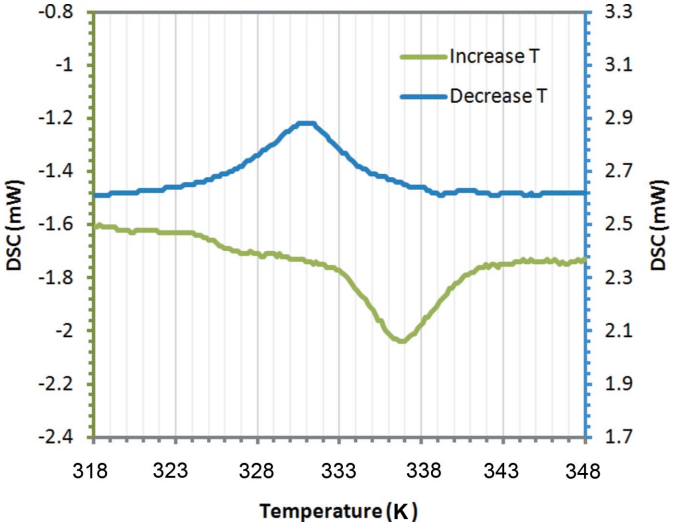

Figure 5
DSC analyses of $TiOF_2$.

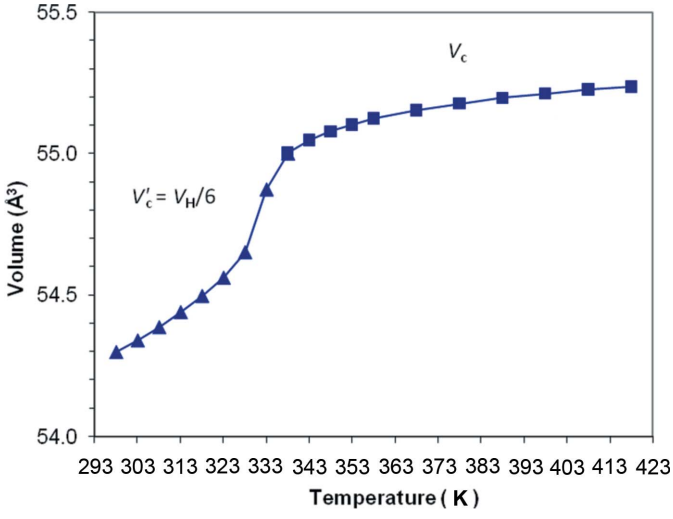

Figure 6
Volume of the $TiOF_2$ unit cell as a function of temperature. V_c' refers to the cubic equivalent volume of a hexagonal unit cell (for temperatures ≤ 333 K).

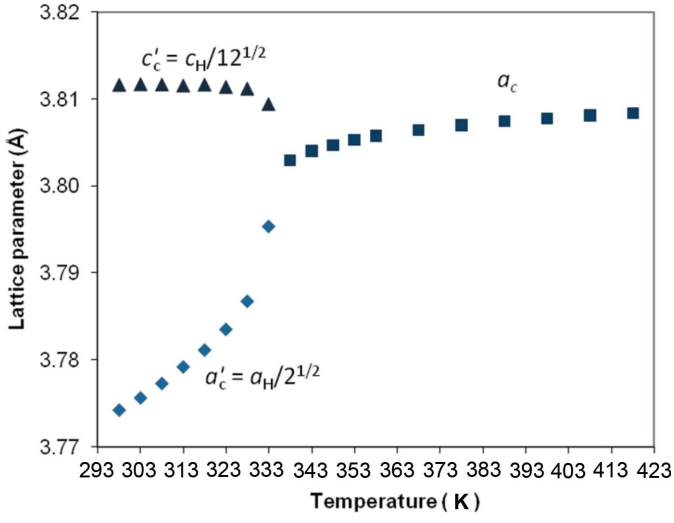

Figure 7
The cubic equivalent lattice parameters of hexagonal (a_c' and c_c') and cubic (a_c) $TiOF_2$ as a function of temperature.

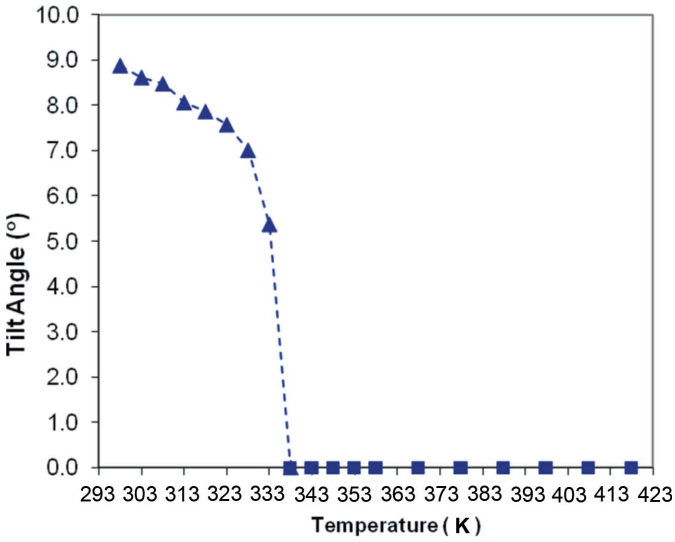

Figure 8
The tilt angle, φ, of the TiO_2F_4 octahedra as a function of temperature.

cubic phase transformation of TiF_3 (Kennedy & Vogt, 2002). The effective ionic radii of O^{2-} and F^- anions are very close in value, *i.e.* 1.40 and 1.33 Å, respectively, for a coordination number of 6 (Shannon, 1976). Hence, the similarities in the structural characteristics observed for $TiOF_2$ in the present work with those of TiF_3 reported by other authors are not unreasonable.

4. Conclusion

Polycrystalline $TiOF_2$ has been formed *via* the metathetic reaction of TiF_4(g) with SiO_2 at 623 K for 4 h. Rietveld analysis of the room-temperature XRD pattern of this reaction product indicated that the $TiOF_2$ possessed a hexagonal unit cell (space group $R\bar{3}c$) with lattice parameters a = 5.3325 (1) Å and c = 13.2321 (4) Å. Upon heating above room temperature, the tilt angle of the TiO_2F_4 octahedra in this hexagonal structure gradually decreased, and the c and a unit-cell lattice parameters decreased and increased, respectively. Continued heating through 333–338 K resulted in the endothermic transformation of $TiOF_2$ from the hexagonal ($R\bar{3}c$) structure to a cubic ($Pm\bar{3}m$) structure. The enthalpy change and structural changes associated with this hexagonal-to-cubic $TiOF_2$ transformation were found to be similar to those previously reported for TiF_3.

This work was supported by the Air Force Research Laboratory (grant No. FA9550-09-1-0162). We thank Dr Robert L. Snyder for helpful discussions.

References

Daniel, P., Bulou, A., Rousseau, M., Nouet, J. & Leblanc, M. (1990). *Phys. Rev. B*, **42**, 10545–10552.
Demourgues, A. & Kempf, J. Y. (2003). French Patent No. 2829482.
Glazer, A. M. (1972). *Acta Cryst.* B**28**, 3384–3392.
Grannec, J., Yacoubi, A., Ravez, J. & Hegenjuller, P. (1988). *J. Solid State Chem.* **75**, 263–269.
Guelin, J., Ravez, J., Grannec, J. & Hagenmuller, P. (1988). *Chem. Scr.* **28**, 137–139.
Gutarra, A., Azens, A., Stjerna, B. & Granqvest, C. G. (1994). *Appl. Phys. Lett.* **64**, 1604–1606.
Hayward, S. A., Morrison, F. D., Redfern, S. A. T., Salje, E. K. H., Scott, J. F., Knight, K. S., Tarantino, S., Glazer, A. M., Shuvaeva, V., Daniel, P., Zhang, M. & Carpenter, M. A. (2005). *Phys. Rev. B*, **72**, 054110.
Howard, C. J., Kennedy, B. J. & Chakoumakos, B. C. (2000). *J. Phys. Condens. Matt.* **12**, 349–365.
ICDD (2007). Card No. 04-007-8589 for $TiOF_2$. International Center for Diffraction Data, Newtown Square, Pennsylvania, USA.
Kennedy, B. J. & Vogt, T. (2002). *Mater. Res. Bull.* **37**, 77–83.
Lee, S. J., Shian, S., Huang, Ch. H. & Sandhage, K. H. (2007). *J. Am. Ceram. Soc.* **90**, 1632–1636.
Lytle, J. C., Yan, H., Turgeon, R. T. & Stein, A. (2004). *Chem. Mater.* **16**, 3829–3837.
Materials Data (2007). *JADE*. Version 8.2. Materials Data Inc., Livermore, California, USA.
Mogus-Milankovic, A., Ravez, J., Chaminade, J. P. & Hagenmuller, P. (1985). *Mater. Res. Bull.* **20**, 9–17.
PANalytical (2006). *X'Pert Highscore Plus*. Version 2.2b. PANalytical, Almelo, The Netherlands.
Poulain, M. & Poulain, M. (1991). *Mater. Sci. Forum*, **67–68**, 129–136.
Reddy, M. V., Madhavi, S., Subba Rao, G. V. & Chowdari, B. V. R. (2006). *J. Power Sources*, **162**, 1312–1321.
Sandhage, K. H. (2006). US Patent 7067104.
Sandhage, K. H., Dickerson, M. B., Huseman, P. M., Caranna, M. A., Clifton, J. D., Bull, T. A., Heibel, T. J., Overton, W. R. & Schoenwaelder, M. E. A. (2002). *Adv. Mater.* **14**, 429–433.
Shannon, R. D. (1976). *Acta Cryst.* A**32**, 751–767.
Shian, S. & Sandhage, K. H. (2009). *Rev. Sci. Instrum.* **80**, 115108.
Tanuma, T., Okamoto, H., Ohnishi, K., Morikawa, S. & Suzuki, T. (2010). *Catal. Lett.* **136**, 77–82.
Unocic, R. R., Zalar, F. M., Sarosi, P. M., Cai, Y. & Sandhage, K. H. (2004). *Chem. Commun.* pp. 796–797.
Vorres, K. & Donohue, J. (1955). *Acta Cryst.* **8**, 25–26.
Vorres, K. S. & Dutton, F. B. (1955). *J. Am. Chem. Soc.* **77**, 2019.
Zhu, J., Zhang, D., Bian, Z., Li, G., Huo, Y., Lu, Y. & Li, H. (2009). *Chem. Commun.* pp. 5394–5396.